NUMERICAL SIMULATION OF STEADY CURRENT BELOW OFFSHORE PIPELINE NEAR PLANE BOUNDARY

Mani Golparvar Fard[1], Abbas Yeganeh-Bakhtiary[2] and Liang Cheng[3]

[1]Postgraduate Student, College of Civil Engineering, Iran University of Science and Technology, Tehran 16844, Iran
[2]Hydro-Structure and Structure Research Center, College of Civil Engineering, Iran University of Science and Technology, Tehran 16844, Iran
[3]School of Civil and Resource Engineering, The University of Western Australia, Perth, Australia

yeganeh@.iust.ac.ir

Abstract: *This paper presents a k-ε turbulence model for simulation of steady current and its induced vortex shedding caused by the presence of an offshore pipeline. Performance of the model around a circular cylinder above a wall with gap to diameter ratios of 0.1, 0.35 and 0.5 under different flow regimes with Reynolds numbers of 1500, 2500 and 7000 is studied. The flow field is computed with solving the Reynolds Averaged Navier-Stokes equations (RANS); the seabed under pipeline is treated as a plane boundary with no-slip boundary condition on pipe surface. The governing equations are solved using Finite Volume Method in a Cartesian coordinate system. Based on the numerical solutions, the flow field, vortex shedding and distribution of shear stress due to the presence of the pipeline near seabed are studied. In addition the mechanism of vortex shedding with different gap to diameter ratios is examined with focusing on the effect of vortex shedding on bed shear stress. It is found that the k-ε turbulence model can well predict the flow field and its induced vortex shedding around a pipeline; hence it can be easily applied for simulation of scour below an offshore pipeline.*

Keywords: *Reynolds averaged navier stokes equations (RANS), k-ε turbulence model, Vortex shedding and local scouring.*

1. INTRODUCTION

Offshore pipelines installed on seabed, have been extensively used as the critical links between offshore fields and storage units. These pipelines disturb the flow field and produce imbalance in local sediment transport that leads to scouring of seabed. As typical cost of offshore pipelines stabilization is in order of millions of US dollars per kilometer in Persian Gulf and Australian West Shelf; hence, the consequences of pipeline failure, would be very sever economically. On the other hand, the flow field and its induced local scour involve a complex turbulent shear flow, which usually interacts with its surrounding bed forms. Therefore, accurate simulation of flow field around a pipeline to account for hydrodynamics forces is very essential.

With these obvious significances, local scour and flow below a pipeline have been subjects of investigation over the last three decades. A series of physical and numerical studies (e.g. Kjeldsen et al. [1]; Mao [2]; Brørs [3]; Sumer and Fredsøe [4, 5, 6], Li and Cheng [7, 8, 9], among others) has been done on local scour below a pipeline. In the numerical studies, it has been found that using different flow models have distinguished effects on the numerical results. Mainly two kind of numerical models for fluid phase in scour prediction below a pipeline have been developed: Former approach is based on the potential flow theory, (see Li and Cheng [10] and Hansen et al. [11]), while the latter one is based on k-ε turbulence model (See Leeuwestein and Wind [12], Brørs [3] and Li and Cheng [8, 9]). It is evident that none of

the studies based on the potential flow models can explain the gentle slope of scour hole formed downstream of a pipeline. This is primarily because the potential flow model is not able to simulate the vortex shedding process associated with the flow around a pipeline. The gentle slope of scour hole is mainly caused by vortex shedding downstream of the pipeline and generates a fluctuating shear stress field on the seabed. The scouring process downstream of pipeline is then affected by the fluctuating shear stress experienced by seabed. As the potential flow model is not capable of simulating this fluctuating stress field; therefore, it cannot simulate the downstream part of the scour hole, (see Sumer et al. [4]).

Early numerical experiments based on the k-ε turbulence model seem to have difficulties with handling seabed deformation caused by scouring. For instance Leeuwestein et al. [12] developed a single-phase numerical model based on k-ε turbulence model. In their numerical part of the investigation, the so-called Cloud in Cell (CIC) method is employed to simulate the flow. It is reported that CIC method generally gives good prediction for the gross characteristics of the organized wake, but the important conclusion is drown that the organized wake behind the pipeline has strong effects on the profile of scour hole; while, time-averaged bed shear stress is not a suitable parameter to use in predicting the Lee-wake scour behind a pipeline. Later on, Van Beek and Wind [13] proposed an improved k-ε turbulence model. In this model, the flow field is obtained by solving the RANS equations with a standard k-ε model. The comparison of the calculation results with the experimental ones is encouraging. Brørs [14] presented a model that includes the description of fluid flow by a standard k-ε turbulence model. Flow around a surface mounted cylinder is predicted in good agreement with the experiments. However, in scour calculations the model does not predict periodic vortex shedding, even during the later stages of scour development.

Li and Cheng [9] developed a numerical model for local scour around pipelines employing a slightly different approach. The flow around the pipeline is solved using a Large Eddy Simulation (LES) model. The results in prediction of seabed shear stress are more accurate than traditional the k-ε turbulence models.

Although numerical modeling of flow around an isolated cylinder has been carried out extensively, only a few studies have considered the flow over a circular cylinder near a plane bed. Lee et al. [15] presented a finite difference solution to 2D Navier-Stokes equations with a Smagorinsky's Subgrid Scale (SGS) turbulence model. In their study, qualitative comparisons show favorable agreement with the experimental measurement of Bearman and Zdravkovich [16], but it is found that the model over-predicts the scour downstream a pipeline, possibly because the 2D-SGS model over predicts the interactions between the vortices shed from the cylinder pipe and seabed. Later, Lei et al. [17] carried out a 2D Direct Numerical Simulation (DNS) in studying wall effect on flow over a circular cylinder for a relatively low Reynolds number; however their study does not contain high Reynolds number in subcritical flow regimes, which induce periodic vortex shedding.

The over prediction of interactions between the vortices shed from pipeline and seabed in previous numerical models, and the lack of numerical models in studying the wall boundary effect on flow for high Reynolds numbers (subcritical regimes of flow) motivated the current research. Therefore, to have more accurate studying of flow field around a pipeline near a plane boundary and to predict interactions among vortices in subcritical regimes of flow, a standard k-ε turbulence model (Launder and Spalding, [20]) is presented. Flow around a circular

cylinder above a wall with gap to diameter ratio of 0.1, 0.35 and 0.5 for different flow regimes with Reynolds numbers (1500, 2500 and 7000) is simulated and the performance of the standard k-ε turbulence model is examined on different steady current motions with different gap ratios.

2. NUMERICAL MODEL

2.1. Governing Equations

The governing equations of the fluid flow are implemented with a vertically two-dimensional turbulence model, as follows:

$$\frac{\partial U}{\partial x}+\frac{\partial V}{\partial y}=0 \tag{1}$$

$$\frac{\partial U}{\partial t}+U\frac{\partial U}{\partial x}+V\frac{\partial U}{\partial y}= -\frac{1}{\rho}\frac{\partial P}{\partial x}+\frac{\partial}{\partial x}\left[2\Gamma\frac{\partial U}{\partial x}\right]+\frac{\partial}{\partial y}\left[\Gamma\left(\frac{\partial U}{\partial y}+\frac{\partial V}{\partial x}\right)\right] \tag{2}$$

$$\frac{\partial V}{\partial t}+U\frac{\partial V}{\partial x}+V\frac{\partial V}{\partial y}= -\frac{1}{\rho}\frac{\partial P}{\partial y}+\frac{\partial}{\partial x}\left[\Gamma\left(\frac{\partial U}{\partial y}+\frac{\partial V}{\partial x}\right)\right]+\frac{\partial}{\partial y}\left(2\Gamma\frac{\partial V}{\partial y}\right) \tag{3}$$

$$\Gamma=\nu+\nu_t \tag{4}$$

in which U, V are mean flow velocity components in streamwise (x) and upward vertical (y) direction, respectively; P is pressure; t is time; Γ is effective viscosity; ν is molecular kinetic viscosity and ν_t is the eddy viscosity.

$$\frac{\partial k}{\partial t}+U\frac{\partial k}{\partial x}+V\frac{\partial k}{\partial y}= \frac{\partial}{\partial x}\left[\left(\nu+\frac{\nu_t}{\sigma_k}\right)\frac{\partial k}{\partial x}\right]+\frac{\partial}{\partial y}\left[\left(\nu+\frac{\nu_t}{\sigma_k}\right)\frac{\partial k}{\partial y}\right]+p_r-\varepsilon \tag{5}$$

$$\frac{\partial \varepsilon}{\partial t}+U\frac{\partial \varepsilon}{\partial x}+V\frac{\partial \varepsilon}{\partial y}= \frac{\partial}{\partial x}\left[\left(\nu+\frac{\nu_t}{\sigma_\varepsilon}\right)\frac{\partial \varepsilon}{\partial x}\right]+\frac{\partial}{\partial y}\left[\left(\nu+\frac{\nu_t}{\sigma_\varepsilon}\right)\frac{\partial \varepsilon}{\partial y}\right]+\frac{\varepsilon}{k}(c_{1\varepsilon}p_r-c_{2\varepsilon}\varepsilon) \tag{6}$$

$$p_r=\nu_t\left[2\left(\frac{\partial U}{\partial x}\right)^2+2\left(\frac{\partial V}{\partial y}\right)^2+\left(\frac{\partial U}{\partial x}+\frac{\partial V}{\partial y}\right)^2\right] \tag{7}$$

$$\nu_t=C_\mu\frac{k}{\varepsilon} \tag{8}$$

in which k is turbulent kinetic energy; ε is dissipation of turbulent kinetic energy; p_r is production of turbulent kinetic energy due to shear stress and C_μ, σ_k, σ_ε, $C_{1\varepsilon}$ and $C_{2\varepsilon}$ are constants for the standard k-ε turbulence model.

Table 1 presents the recommended values for the model constants according to Launder and Spalding [20].

Table1. Constants for the standard *k-ε* turbulence model.

c_μ	σ_k	σ_ε	$c_{1\varepsilon}$	$c_{2\varepsilon}$
0.09	1.0	1.3	1.44	1.92

2.2. Computational Domain

Fig. 1 gives a sketch of the computational domain. The water depth is considered equal to 3.5D, which is chosen on the fact that vortex shedding in this case, is not as crucial as that of the behind an isolated cylinder while the gap ratio (e/D) is small. Horizontal distances are set to 10D for the upstream and 20D for the downstream lateral boundaries. These distances are chosen on the basis that less distance may cause the outflow and inflow boundary conditions to highly affected by both vortex shedding and stream traces of the fluid phase. It is known that while the gap ratio is less than 0.3, vortex shedding would be totally suppressed; therefore to have a precise study of gap ratio effects on vortex shedding, different gap to

diameter ratio has been used in this study. Hence the computation domain would cover from x/D=-10 to x/D=20 in the horizontal direction and from y/D=0 to y/D=3.5 in the vertical direction. The cylinder is placed with its center in (x, y)=(10D, e); while "e" is 0.1D, 0.35D or 0.5D.

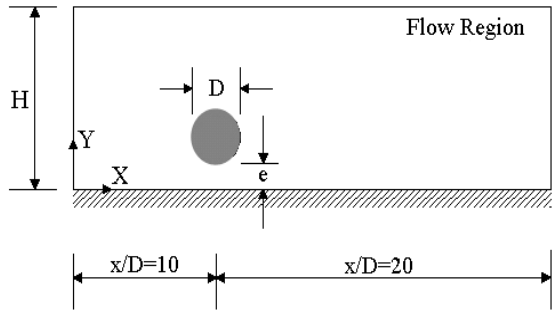

Fig. 1. Sketch of flow domain and its boundary conditions.

2.3. Boundary Conditions

At the water surface, a symmetric boundary condition is applied as follows:

$$\frac{\partial U}{\partial y} = 0, \quad V = 0 \tag{9}$$

At solid boundary (i.e. pipe surface), the no-slip boundary condition normal to its surface is employed:

$$U = 0 \text{ or } V = 0 \tag{10}$$

For seabed boundary, the wall function is implemented, namely the logarithmic law holds between solid wall and its adjacent grid point. On later stages of scour simulation, for proper fitting of logarithmic velocity distribution, the theoretical bed level would be set below the average height of the particles surface, (see Yeganeh et al. [21]). The boundary condition for streamwise velocity, at the grid point ($y=y_p$) in the vicinity of bottom is expressed as:

$$\begin{cases} \dfrac{U(y_p,t)}{U_*} = \dfrac{y_p U_*}{\nu} & \dfrac{y_p U_*}{\nu} \le 11.63 \\ \dfrac{U(y_p,t)}{U_*} = \dfrac{1}{\kappa}\ln(9.793\dfrac{y_p U_*}{\nu}) & \dfrac{y_p U_*}{\nu} > 11.63 \end{cases} \tag{11}$$

in which κ is von-Kármán constant (=0.41) and U_* is shear velocity.

An additional assumption of the local equilibrium between generation and dissipation of turbulent energy is made at the grid point in the vicinity of bottom wall, hence k and ε at the first grid are calculated by

$$k = \frac{U_*^2}{\sqrt{C_\mu}} \quad ; \quad \varepsilon = \frac{U_*^2}{\kappa y_p} \tag{12}$$

3. NUMERICAL EXPERIMENTS AND DISCUSSION:

To demonstrate the effect of vortex shedding on bed shear stress and its effect on local scour, flow around a circular cylinder above a fixed plane is simulated using a standard k-ε turbulence model. It is apparently evident that the fluctuating shear stress due to vortex shedding around a pipe has a key effect in the local scour around it as through using physical model tests, Sumer et al. [4] observed that the near-bed velocity fluctuates significantly downstream of the model pipe. Therefore, it is suggested that the fluctuating seabed shear stress has a physically powerful effect on the local scouring downstream of the pipe and consequently, in this study, it has been considered for modeling of flow below a pipeline and its induced local scour.

When a cylinder is located near a wall, it is expected that vortex shedding depends on the Reynolds number (Re), the gap ratio (e/D) and the characteristics of wall boundary layer. Generally, vortex shedding occurs when the Reynolds number, Re, based on the cylinder diameter (D) and the free-stream velocity (U) is above 40. For the Reynolds numbers up to above 150, the vortex shedding flow remains laminar (See Beaudan and Moin [23]). Transition to three-dimensional flow starts at a Reynolds number of about 180-194 depending on experimental conditions, and ends at about Re= 260, at which fine scale three-

dimensional eddies appear (See Williamson [24]). Furthermore the flow is classified as subcritical regime for Reynolds number from 300 to 1.4×10^5 (see Niemann and Hölscher [25]). It is in this subcritical regime of flow that the boundary layer along the cylinder surface is laminar throughout the circumference until separation and periodic vortex shedding would be induced.

Therefore in this study, to insure the vortex shedding situations thoroughly tested, the Reynolds numbers are taken in the range of the subcritical regime values (1500, 2500 and 7000). To diminish the effect of mesh size on numerical solution and to brace the Cartesian coordinate system, a careful mesh-independence study has been done, and as a result a 602×72 mesh with grid points being concentrated toward flow direction and the seabed is employed for cases studied, (Fig. 2).

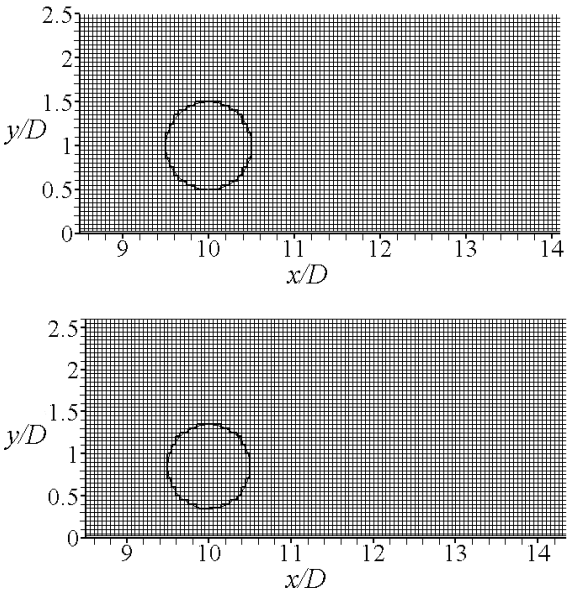

Fig. 2. Computational Mesh for e/D= 0.35 and e/D= 0.5.

3.1. Observing Flow Field

To understand the flow field characteristics and the mechanism of vortex shedding due to the presence of pipe near seabed, Figs. 3 and 4 are presented. The process of vortex shedding around pipe and the interaction of vortices with the seabed are clearly displayed by the velocity vectors depicted in these figures.

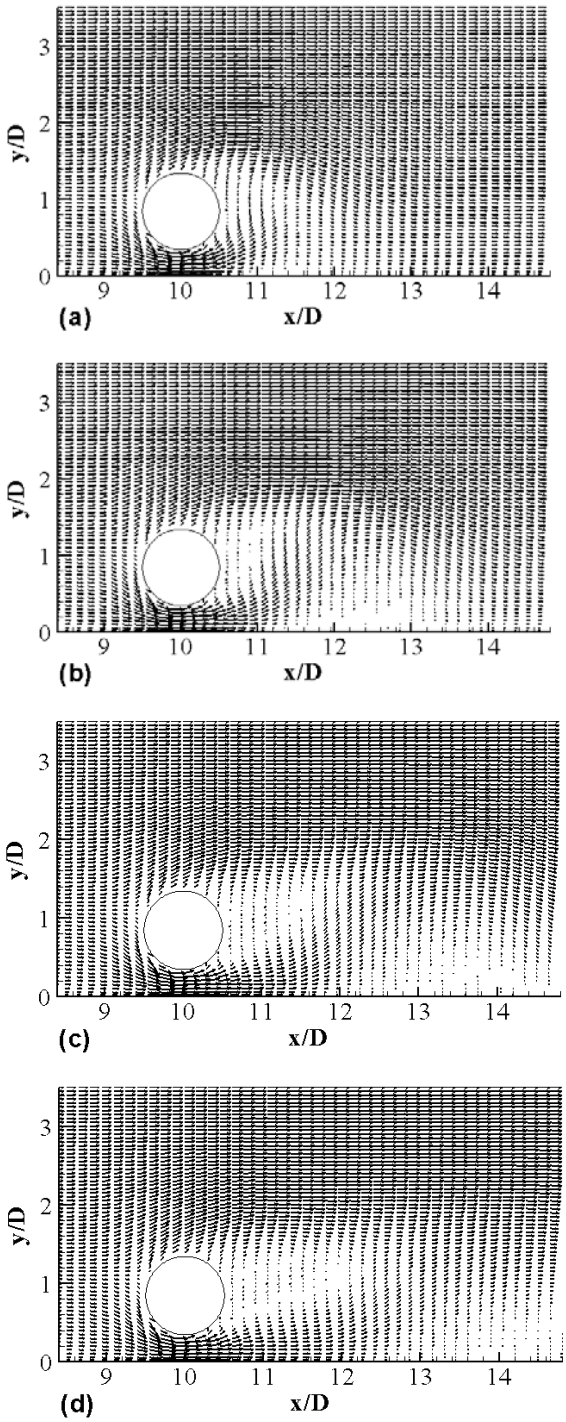

Fig. 3. Flow pattern during vortex shedding process (e/D = 0.35, Re=1500).

Two different gap ratio parameters (0.35 and 0.5) for Reynolds number of 1500 are

presented. It is readily seen that: (i) vortices are shed alternatively from the top and bottom, forming a vortex street downstream of the pipe; and (ii) there are clearly interactions between seabed and vortices shed from the pipe especially when the gap ratio is 0.35, which allows more interaction between pipe and seabed.

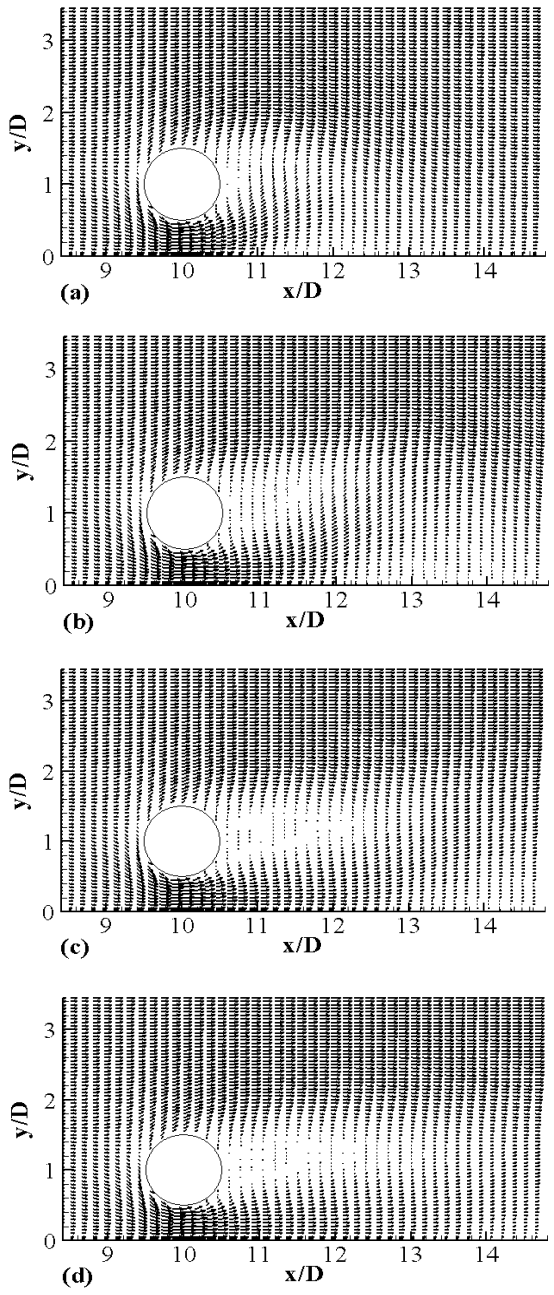

Fig. 4. Flow pattern during vortex shedding process (e/D = 0.5, Re=1500).

3.2. Mechanism of Vortex Shedding

To understand the mechanism of vortex shedding at different gap ratios, it is useful to look at the vortex shedding formations first. Figs. 5, 6 and 7 present the instantaneous vorticity contours calculated in one shedding cycle at Re= 1500 and e/D= 0.1, 0.35 or 0.5, respectively.

In the vicinity of cylinder and wall, there are three layers of velocity, two shear layers that develop along on the top and bottom surface of the cylinder, and a shear layer develops along the wall. These three layers are clearly visible in Figs. 5, 6 and 7. Both the top shear layer on the cylinder and the shear layer on the wall induce a strong vorticity, while the vorticity changes sign from negative to positive as the layer is changed. The formation or suppression of the vortex shedding results from the interaction of these three layers, can be described as follows:

At Fig. 5a, the tail of a positive vortex is being formed and it is being fed by the lower shear layer at the bottom of cylinder. In the meantime, a negative vortex is forming from the upper shear layer. For the time being, in Fig.5b, the feeding of negative vortex from the upper shear layer is cut off by growing positive vortex; while, the newly formed negative vortex downstream of the pipe continues to grow and pushes the positive vortex downstream. This process is quite significant as it passes through Fig. 5c and continues through Fig. 5d. It is due to instability in the lower free shear layer resulting from a high concentration of positive vorticity that the lower shear layer rolls up to form a positive vortex. The formation procedure of vortex continues, so that it reaches to a steady periodic vortex shedding process.

As the gap to diameter ratio (e/D) is changed to 0.5, the wall shear layer at the cylinder location places far from the lower shear layer on the cylinder surface (Fig. 6). Therefore in the vortex formation area, these two shear

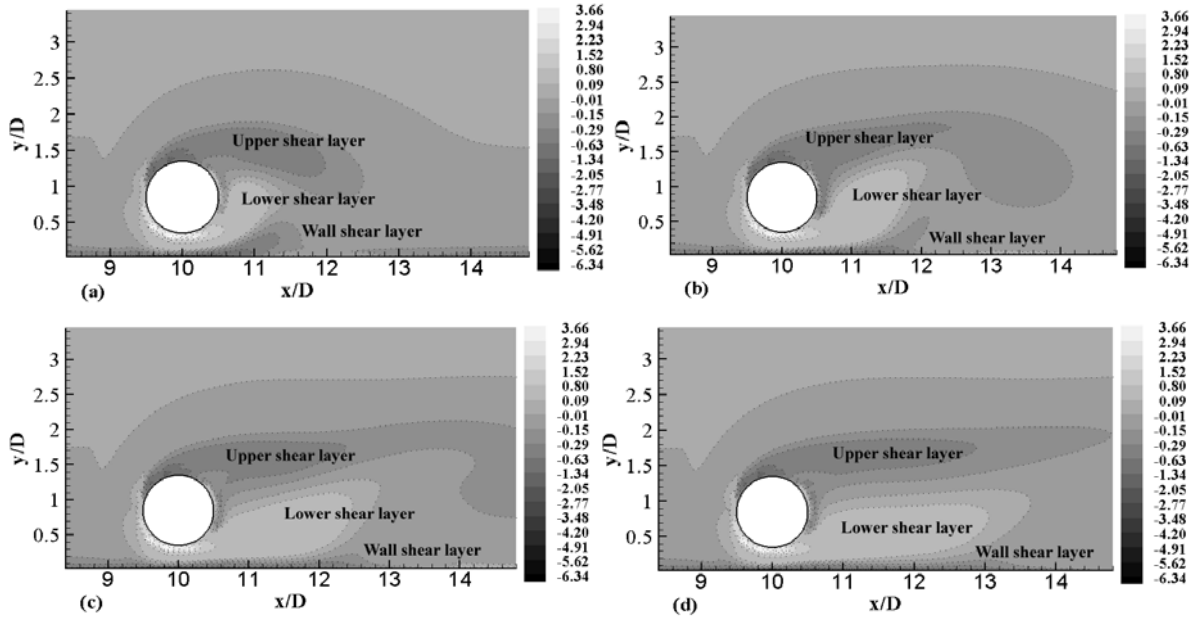

Fig. 5. Instantaneous vorticity around a pipeline, (D= 100 mm, e/D= 0.35, U= 150 mm/s).

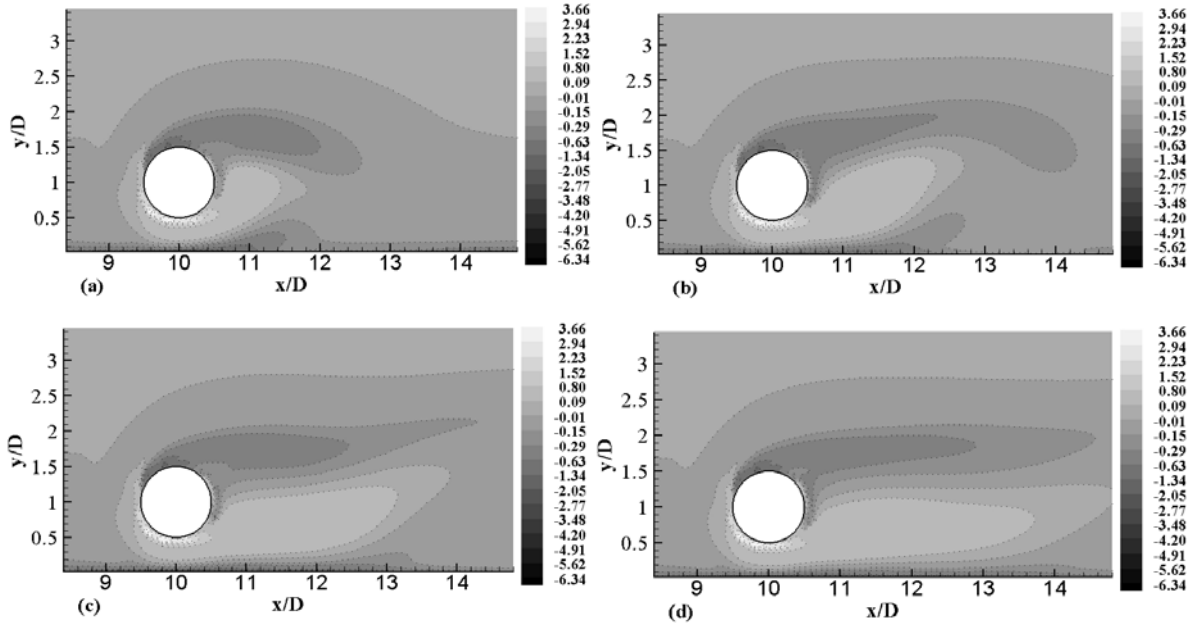

Fig. 6. Instantaneous vorticity around a pipeline, (D= 100 mm, e/D= 0.50, U= 150 mm/s).

layers do not interact on the cylinder surface. As the wall shear layer grows, it separates from wall at a location downstream of the pipe and forms a negative vortex. This negative vortex gets together with a vortex pair resulted from the vortex shedding and mixes the negative vortex originating from the top of the cylinder in far wake, while they are transporting downstream. It is concluded that due to the significant distance between the pipe and seabed, the vortex shedding does not get affected by the shear wall layer at this gap ratio.

The situation changes considerably at very small gap ratios. Fig. 7 demonstrates the instantaneous vorticity contours for the same

Reynolds number. Due to the small gap between the pipe and seabed (e/D= 0.1), vorticity in the separated free shear layer gets very week; therefore, the upper shear layer continues to grow and affect downstream, without forming any vortices in the near wake of the pipe. In this condition, the near wake is quite stable since no vortex shedding is formed.

3.3. Effects of Reynolds Number

Figs. 6, 8 and also 9 present the instantaneous vorticity contours obtained at Reynolds numbers (Re= 2500 and 7000).

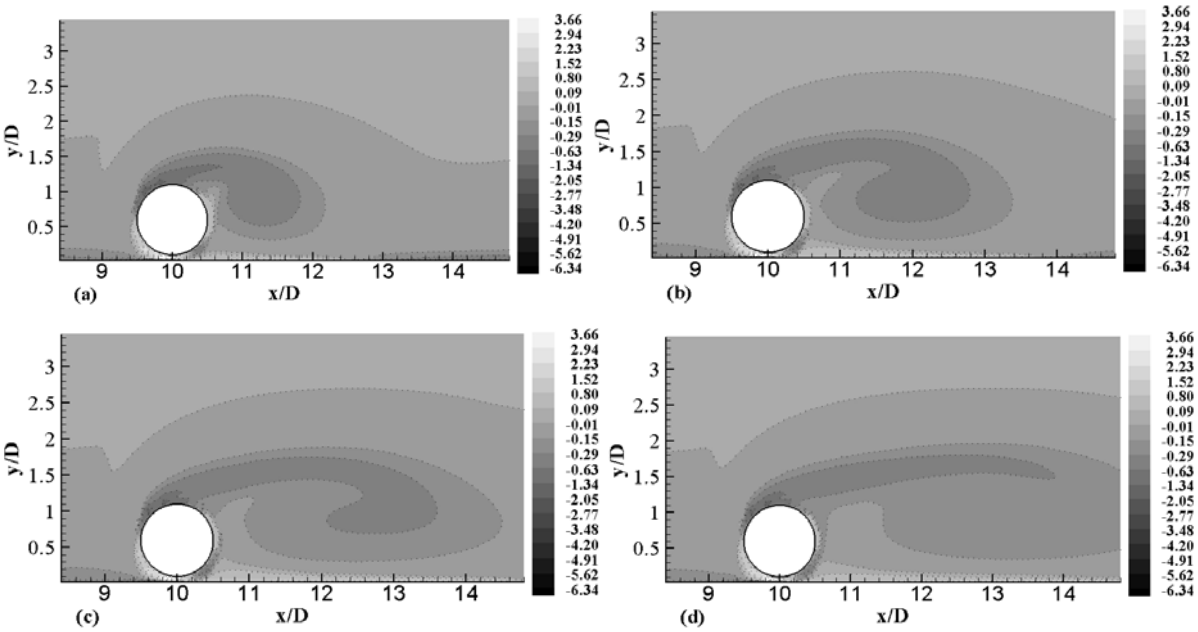

Fig. 7. Instantaneous vorticity around a pipeline, (D= 100 mm, e/D= 0.10, U= 150 mm/s).

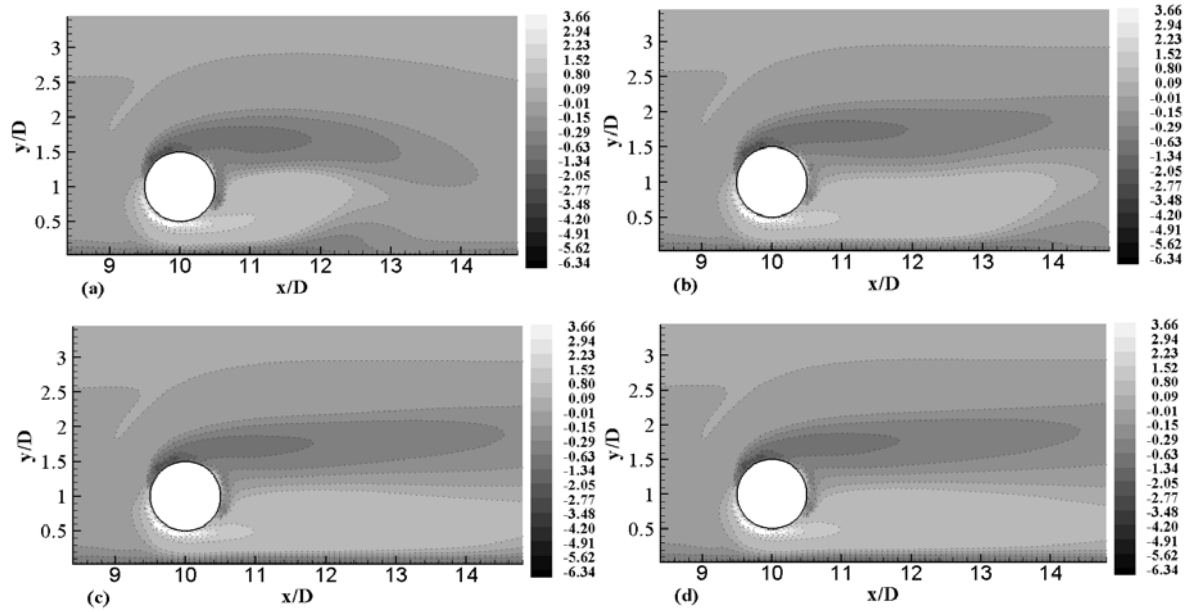

Fig. 8. Instantaneous vorticity around pipeline, (e/D= 0.50, U= 250 mm/s, Re=2500).

To minimize the effect of gap to diameter ratio, e/D is set to 0.5. In this gap to diameter ratio, the wall shear layer at the cylinder location places far from the lower shear layer on cylinder surface and it would be possible to observe the effect of Reynolds numbers apart of gap to diameter ratio.

Comparing to low Reynolds numbers regimes of flow reported by Lei et al. [17], the overall vorticity level in shear layers in high Reynolds numbers are higher and three shear layers are thinner that those at low Reynolds numbers. The effect of different high Reynolds numbers can be observed through Figs. 6, 8 and 9 as Re increases from 1500 to 7000. When Re reaches 7000, wall shear layer at the cylinder is almost annihilated and due to its weak performance, it is not able to roll up and form vortices; consequently, it would not interact with other two layers.

A pair vortex resulted from the cylinder is observed in all situations. This pair vortex would not interact on the cylinder surface but it would mix the negative vortex originating from the top of the cylinder in far wake; while, they are transporting downstream. Consequently, these upper and the lower free shear layers forming the pair vortex are transported downstream; thus, the wake development can be easily seen.

3.4. Characteristic of Bed Shear Stress

Amplitude of shear stress oscillation and the mean values of shear stress vary at different locations along seabed. To observe such variations, Fig. 10 gives the distribution of the values of the seabed shear stress along seabed downstream of pipeline. It can be easily seen that the maximum shear stress takes place directly underneath of pipe with large amplitude of oscillation as Reynolds number changes. It can also be observed that the maximum bottom shear stress reaches its second peak at distance almost equal 5-7 pipe diameters downstream of the pipe and decreases again as it moves downward, especially when gap to diameter ratio (e/D) is 0.1. The similar phenomenon was observed by Sumer et al. [4] in their physical experiments, where the velocity oscillations near the seabed were employed to discuss the effect of vortex shedding on the local scour.

The second peak in seabed shear stress is due to small gap ratio between the cylinder and the seabed and it is significant as normally it

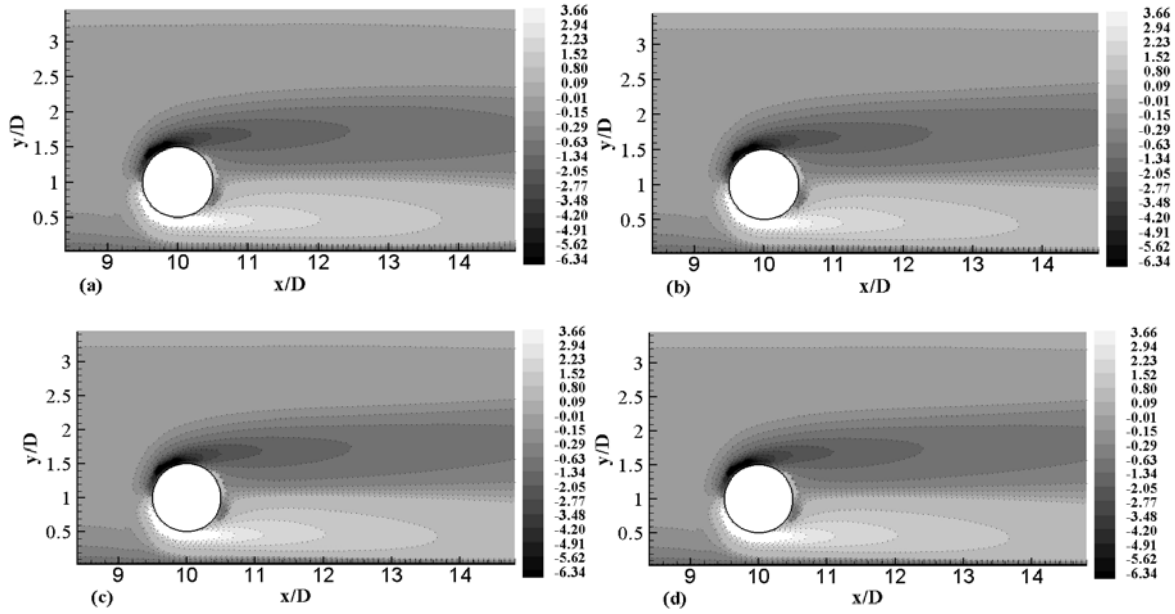

Fig. 9. Instantaneous vorticity around pipeline, (e/D= 0.50, U= 700 mm/s, Re=7000).

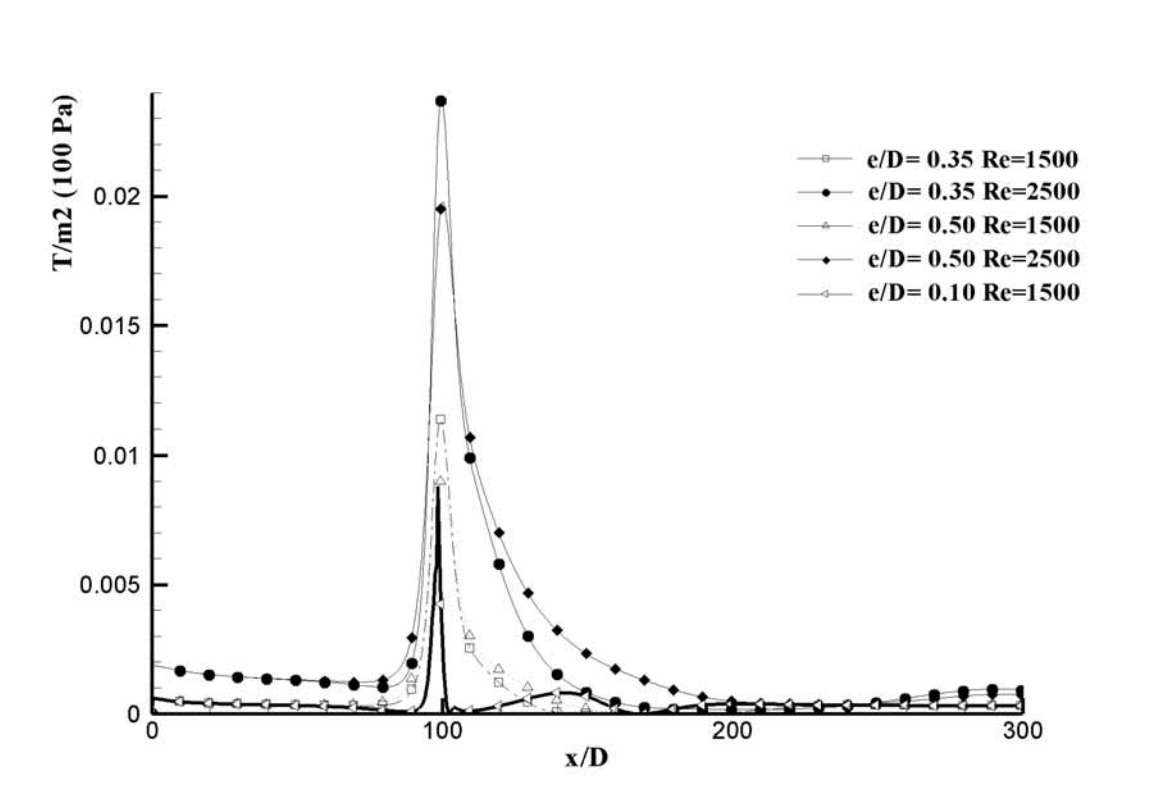

Fig. 10. Characteristic Bed shear stresses (D=100 mm, Fixed Flat Bed).

is in this region that strong scouring can be observed. It is concluded that a domain of at least 7 diameters downstream of the pipe is needed to model local scour under offshore pipeline.

4. CONCLUSIONS

The following conclusions can be drawn:

- A standard k-ε turbulence model with the so-called wall function boundary condition is computationally affordable and relatively well calibrated for different Reynolds-Number engineering flows, in addition comparing to experimental visualizations, numerical visualization can provide more details about the flow field, Thus the mechanism of vortex shedding in steady current due to the presence of pipe near seabed can be easily observed.
- Reynolds number has a significant effect on vortex shedding caused by the presence of the pipe. Only in subcritical regime, the boundary layer along the surface of the cylinder is laminar throughout the circumference until separation.
- At small e/D, as a result of the contact of these shear layers, the positive vorticity in the lower shear layer is cancelled by the negative vortex forming at the wall shear layer. Consequently, the lower shear layer is suppressed and it would not be strong enough to roll up and form vortices; therefore it would not have any significant effect on the upper shear layer. As e/D increases, the vortex shedding is more observable and the vorticity phenomena would be enhanced by increase in Reynolds number.
- Compared to the low Reynolds number flows, the overall vorticity level in shear layers in high Reynolds numbers are higher and three shear layers are thinner that those at low Reynolds numbers**.** Whereas in high Reynolds numbers, the wall shear layer at cylinder is almost defeated and it would not

able to roll up and form vortices; consequently, it would not interact with other two shear layers. The pair vortex resulted from the cylinder would not interact on the cylinder surface but while transporting downstream, they would mix the negative vortex originating from the top of the cylinder in far wake, therefore, the wake development can be easily seen.

- Seabed shear stress has a significant effect on local scour under offshore pipelines and it is easily seen that due to the presence of pipe, the scour hole caused by the vortex shedding can be enlarged even to 5-7 diameters downstream of the pipe.
- Instead of using curvilinear coordinate systems, the present study uses a Cartesian coordinate system for simulation of flow field around the pipe. In order to have a precise study, a mesh-independence study has been done, and a dense mesh with grid points being concentrated toward flow direction and the seabed is employed for cases studied. This coordinate system suffers from heavy load of numerical calculations; even though the level of precision is not significantly changed. Using curvilinear coordinate systems with grid points being concentrated toward pipe surface and the seabed would lessen the amount of numerical solutions.

REFRENCES

[1]. Kjeldsen, S.P., Gjørsvik, O., Bringaker, K.G. and Jacobsen, J., 1973. Local scour near offshore pipelines. Proceeding of Second International Conference on Ports and Ocean Engineering under Arctic Conditions, University of Iceland, pp. 308-331.

[2]. Mao, Y., 1986. The interaction between a pipeline and erodible bed. PhD Dissertation, Technical University of Denmark, Lyngby, Denmark.

[3]. Brørs, B., 1999. Modeling of flow and scour at pipelines. Journal of Hydraulic Engineering 125 (5), pp. 511–523.

[4]. Sumer, B.M. and Fredsøe, J., 1988. Interaction between vibrating pipe and erodible bed. Journal of Waterway, Port, Coastal and Ocean Engineering. ASCE 114, 5, pp. 599–614.

[5]. Sumer, B.M. and Fredsøe, J., 1992. A review of wave/current-induced scour around pipelines. Proceeding of 23rd Int. Conference on Coastal Eng. (ICCE 1992), Chapter 217, pp. 2839–2852.

[6]. Sumer, B.M. and Fredsøe, J., 1999. Wave scour around structures. Advanced Coastal and Ocean Engineering, Editor Philip, L.-F., Liu, (4), pp. 191-249.

[7]. Li, F. and Cheng, L. 1998. Numerical simulation of local scour under offshore pipelines. Proceeding of 8th International Conference on Offshore and Polar Eng., ISOPE`98, Vol. 2, pp. 76-81.

[8]. Li, F. and Cheng, L., 1999. A numerical model for local scour under offshore pipelines. Journal of Hydraulic Engineering, ASCE 125, 4, pp. 400- 406.

[9]. Li, F. and Cheng, L., 2000. Towards prediction time development of local scour around offshore pipelines. International Symposium on scour of foundations, The international Society on Soil Mechanics and Geotechnical Engineering (ISSMEG), Melbourne, Australia, pp. 103-117.

[10]. Li, F. and Cheng, L., 2001. Prediction of lee-wake scouring of pipelines in currents. Journal of Waterway, Port, Coastal and Ocean Engineering, ASCE 127, pp. 106-112.

[11]. Hansen, E. A., Fredsøe, J., and Ye, M. 1986. Two-dimensional scour below pipelines. Proc. of 5th Int. symposium on offshore mechanics and arctic eng, ASCE, New York, pp. 670–678.

[12]. Leeuwestein, W., Bijker, E. A.,

Peerbolte, E. B., and Wind, H. G. 1985. The Natural self burial of submarine pipelines. Proceeding 4th International Conference on behavior of Offshore structures (BOSS), Elsevier Science, New York, pp. 717-728.

[13]. Van Beek, F. A., and Wind, H. G. 1990. Numerical modeling of erosion and sedimentation around pipelines. Journal of Coastal Engineering. Vol. 14, pp. 107-128.

[14]. Brørs, B., 1999.Numerical Modeling of Flow and Scour at Pipelines. Journal of Hydraulic Engineering, Vol. 125, No. 5, pp. 511-523.

[15]. Lee, Y. G., Hong S. W., Kang, K. J., 1994. A numerical simulation of vortex motion behind a circular cylinder above a horizontal plane boundary. Proceeding of the Fourth International Offshore and Polar Engineering Conference, Osaka, Japan, Vol.3, pp. 427–433.

[16]. Bearman, P. W., Zdravkovich, M. M., 1978. Flow around a circular cylinder near a plane boundary. Journal of Fluid Mechanics 89 (1), pp. 33-47.

[17]. Lei, C., Cheng, L., Kavanagh, K., 1999a. A finite difference solution of the shear flow over a circular cylinder. Ocean Engineering 27 (3), pp. 271-286.

[18]. [18] Lei, C., Cheng, L., Kavanagh, K., 1999b. Reexamination of the effect of a plane boundary on force and vortex shedding of a circular cylinder. Journal of Wind Engineering and Industrial Aerodynamics 80 (3), pp. 263-286.

[19]. Jensen, B. L. 1987. Large-scale vortices in the wake of a cylinder placed near a wall. Proceeding of Second International conference on laser anemometry-advanced and applications, Strathcyde, UK, pp. 153–163.

[20]. Launder, B. E., Spalding, D. B., 1974. The numerical computation of turbulent flows. Computer Methods in Applied Mechanics and Engineering (3), pp. 269-289.

[21]. Yeganeh-Bakhtiary, A., Gotoh, H. and Sakai, T. 2000a. Numerical Study of the Euler-Lagrange coupling multiphase flow model to the bed-load transport at high shear stress. Journal of Hydraulic Research, IAHR, Vol. 38, 5, pp. 389-398.

[22]. Grass, A. J., Raven P. W. J., Stuart, R. J., Bray, J. A, 1984. The influence of boundary layer velocity gradients and bed proximity on vortex shedding from free span pipelines. Journal of Energy Resources Technology, 106, pp. 70-78.

[23]. Beaudan, P. and Moin, P., 1994. Numerical experiments on the flow past a circular cylinder at subcritical Reynolds number, Report No.TF-62, Thermosciences Division, Department of Mechanical Engineering, Stanford University, Stanford, California, USA.

[24]. Williamson, C. H. K., 1996. Vortex dynamics in the cylinder wake. Annual Review of Fluid Mechanics 28, pp. 477-539.

[25]. Niemann, H. J., Hölscher, N., 1990. A review of recent experiments on the flow past circular cylinders. Journal of Wind Engineering and Industrial Aerodynamics 33, pp. 197-209.